Widespread biological response to rapid warming on the Antarctic Peninsula

Matthew J. Amesbury[1*], Thomas P. Roland[1], Jessica Royles[2,3], Dominic A. Hodgson[3], Peter Convey[3], Howard Griffiths[2], Dan J. Charman[1]

[1] Geography, College of Life and Environmental Sciences, University of Exeter, Exeter, Devon, EX4 4RJ, UK.

[2] Department of Plant Sciences, University of Cambridge, Cambridge, Cambridgeshire, CB2 3EA, UK.

[3] British Antarctic Survey, Cambridge, Cambridgeshire, CB3 0ET, UK.

[*] Correspondence and lead contact: m.j.amesbury@exeter.ac.uk

Summary

Recent climate change on the Antarctic Peninsula is well documented [1–5], with warming, alongside increases in precipitation, wind strength and melt season length [1,6,7], driving environmental change [8,9]. However, meteorological records mostly began in the 1950s and paleoenvironmental datasets that provide a longer-term context to recent climate change are limited in number and often from single sites [7] and/or discontinuous in time [10,11]. Here we use moss bank cores from a 600 km transect from Green Island (65.3°S) to Elephant Island (61.1°S) as palaeoclimate archives sensitive to regional temperature change, moderated by water availability and surface microclimate [12,13]. Mosses grow slowly but cold temperatures minimise decomposition, facilitating multi-proxy analysis of preserved peat [14]. Carbon isotope discrimination ($\Delta^{13}C$) in cellulose indicates the favourability of conditions for photosynthesis [15]. Testate amoebae are representative heterotrophs in peatlands [16–18] so their populations are an indicator of microbial productivity [14]. Moss growth and mass accumulation rates represent the balance between growth and decomposition [19]. Analysing these proxies in five cores at three sites over 150 years reveals increased biological activity over the past ca. 50 years, in response to climate change. We identified significant changepoints in all sites and proxies, suggesting fundamental and widespread changes in the terrestrial biosphere. The regional sensitivity of moss growth to past temperature rises suggests that terrestrial ecosystems will alter rapidly under future warming, leading to major changes in the biology and landscape of this iconic region; an Antarctic greening to parallel well-established observations in the Arctic [20].

RESULTS

Moss banks are regional palaeoclimate archives

Moss banks are distributed sporadically along the western Antarctic Peninsula (AP) [21] from Alexander Island (69.4°S) [14] to Elephant Island (61.1°S) (Figure 1; Table S1) and north-east to Signy Island, South Orkney Islands (60.7°S) [15]. Mosses accumulate in small annual increments from new

growth at the surface and old moss growth is exceptionally well-preserved [22] by year-round cold temperatures and relatively rapid incorporation into permafrost, leading to deep accumulations of moss over thousands of years. AP moss banks are often dominated by a single species (*Polytrichum strictum* or *Chorisodontium aciphyllum*) and are easily dated by radiocarbon due to their highly organic nature [13]. Relatively stable down-core bulk density and peat humification profiles (Figure S4, see also [14]) show that compaction or decomposition effects are not significant. Mass accumulation (r^2 = 0.82, p = 0.013) and growth rates (r^2 = 0.75, p = 0.026) are significantly positively related to latitude but since latitudinal temperature variability over our study area is not significant (Figure 1; [23,24]), these trends are likely driven by differences in the dominant moss species (Table S1). Therefore, moss bank proxies provide unique insights into the scale and rapidity of biological shifts over decadal to centennial timescales in the past and under future warming.

A widespread biological response

We found significant changes in all proxies (carbon isotope discrimination, microbial productivity, moss bank vertical growth and mass accumulation) and at all sites, reflecting increased biological activity across the length of the AP over the past ca. 50 years (Figures 2 and 3). The precise timing of these shifts varied, but the prevalent pattern of change indicates a widespread biological response to increasing temperature. We identified significant changepoints (confidence value >0.98) in 20 of 23 time series (Figure S1), suggesting that all four proxies have undergone fundamental state changes in recent years. An alternative method for changepoint detection produced similar results with a mean difference in ages between the two methods of 13 years (Figure S2). The three $\Delta^{13}C$ time series in which changepoints were not identified (ELE3, ARD1, GRE1) still showed trends of increasing discrimination consistent with other sites/cores/proxies within the past ~50 years (Figure S2). In two cases (ARD1, GRE1), there were more recent $\Delta^{13}C$ declines to lower discrimination that, combined

with the higher growth rates, suggests sub-optimal growth conditions over a longer annual growing period [15]. A trend to lower discrimination was also observed in one core (GRE2) where the post-changepoint state was negative, suggesting poorer conditions for photosynthesis at this site. Summary changepoint data show that a majority of state changes occurred after 1950 (Figure 3). To investigate whether there was a significant difference before and after AD 1950 that was prevalent across the whole of the AP, we compared pre- and post-1950 states, averaged across all sites/cores (Figure 4). There was an observable difference for all proxies apart from $\Delta^{13}C$.

DISCUSSION

Palaeo-data are key to AP climate debates

The value of palaeo-data in understanding Antarctic climate is highlighted by the limitations of instrumental and satellite records, which alone are not sufficient to determine whether recent trends are anthropogenically forced or remain within the range of natural climate variability [25,26]. Ice core records indicate that warming over the past century is highly unusual in the context of natural variability over the past 2000 years [27]. Observational records show that the physical [28–30] and ecological [9,10] effects of 'recent rapid regional' [3,31] warming since the 1950s on the AP have been significant. However, this evidence has often been obtained from a single site [7] at a single trophic level, or is discontinuous in time [10,11], meaning that a 'baseline' ecological state has not been established and used to evaluate recent change and the likely sensitivity of future ecosystem responses [32]. In addition, the spatial heterogeneity of ecological responses to climate change makes it difficult to extrapolate from local, short-term studies of individuals and populations to an ecosystem level response to wider climatic trends [33]. Given the large interannual and decadal variability in Antarctic climate, placing recent short-term observational records in a longer-term context is important to determine and differentiate the roles of natural variability and anthropogenic forcing [34]. Our multi-proxy dataset over 150 years from moss bank cores spanning a 600 km

latitudinal transect addresses these issues and enables a robust assessment of regional variability over time.

Drivers of rapid change

Our data indicate a widespread biological response to recent rapid warming on the AP. The extent of the site network and multi-proxy approach show that spatial and temporal variability, across multiple trophic levels, is small in relation to overall trends (Figure 2) such that we can have confidence in the overall widespread nature of the observed biological response to recent warming. However, the detailed patterns of change in individual proxies, particularly in $\Delta^{13}C$, allow further analysis of the response to microclimatic and microtopographic conditions specific to each moss bank location [12].

Abrupt shifts in microbial population change, growth and mass accumulation rates were found in all cores, with significant differences between pre- and post-changepoint states (Figure 2). This suggests that moss banks have responded not only to gradual warming [35] (Figure 1), but that rapid changes can also occur across thresholds, which may not be temperature driven (for example, moisture availability during the growing season). Water availability is a key control on the growth rates and activity of Antarctic terrestrial organisms [36], including mosses and soil protozoa [14]. Free water availability is likely to have increased over the AP since the 1950s in concert with trends in temperature, precipitation and growing season length [1,6], but is governed by spatially heterogeneous precipitation trends and site-specific (micro)topography to a greater extent than temperature. Moisture availability may also increase in the future as a result of poleward contraction of westerly winds and increased meridional circulation [4,37].

123 $\Delta^{13}C$ data support the hypothesis that the moisture status during periods of net photosynthetic
124 assimilation has been spatially and temporally variable, with differences in $\Delta^{13}C$ both between and
125 within sites. Measured $\Delta^{13}C$ values indicate the optimality of conditions for photosynthesis,
126 integrated over the growing period [13,15]. High $\Delta^{13}C$ values are associated with minimal diffusion
127 limitation for CO_2 at the tissue surface and therefore drier conditions [38]. Wind conditions,
128 evaporation and surface microtopography as well as temperature and precipitation all affect surface
129 leaf level surface moisture. Long, damp seasons can result in high growth rates but low $\Delta^{13}C$ values,
130 whilst warm, dry periods can result in an instantaneously high $\Delta^{13}C$ before desiccation ends
131 assimilation and little biomass is preserved. In general, $\Delta^{13}C$ increased between the 1970s and 2000,
132 in concert with rising temperatures and likely improving conditions for photosynthesis, prior to a
133 recent decline. Reduced $\Delta^{13}C$ since around 2000 coincides with the cessation of warming [4] and,
134 potentially, reduced evaporation. The two Green Island cores, taken from within 100m, show
135 contrasting patterns, with GRE1 following the general trend of a non-significant increase in $\Delta^{13}C$
136 preceding a recent decline, whereas GRE2 shows a significant drop in $\Delta^{13}C$ around 1965. As
137 precipitation, temperature and wind are similar between the two core sites, a more local control is
138 likely. For example, changes in microtopography at GRE2 may have resulted in surface water pooling
139 where mosses were still able to photosynthesise and grow, but CO_2 diffusion and therefore $\Delta^{13}C$ were
140 reduced.
141
142 The strong response of moss growth and microbial populations to increasing temperature, coupled
143 with the $\Delta^{13}C$ results, suggest that these systems are driven primarily by temperature, strongly
144 modified by more localised changes in water availability at both regional and local scales. Increasing
145 temperature has likely driven a longer growing season and a greater number of days in the year
146 where air temperature at the moss surface exceeds 0°C for at least part of the day. The largest
147 increases in recorded temperature have occurred during the winter, spring and autumn periods [34],

148 which suggests that changing temperature has had the greatest impact on biological productivity
149 during the shoulder periods of the growing season. Thus, whilst longer periods of growth have
150 resulted in overall higher growth rates and increased microbial productivity, the changes in $\Delta^{13}C$
151 suggest that growing conditions at any point in time may actually have been worse, likely due to
152 sub-optimal moisture availability. There is some suggestion (Figure 2) that very recent growth rates
153 of moss and microbial populations may have been slower and this could be the result of lack of
154 moisture or a reversal in the direction of temperature change in some parts of the year [4].
155
156 **Future terrestrial biological change**
157 There is no doubt that biological responses to temperature variation on the AP have been rapid and
158 that large shifts in the ranges and growth rates of mosses and microbial communities can be
159 expected if recent rates of temperature change increase, as predicted, even recognising the current
160 reversal of warming in this region [1,4], and associated environmental changes such as glacier retreat
161 [30] continue. Biological activity measured as moss growth or mass accumulation rates has increased
162 4-5 fold between pre- and post-changepoint states (Figure 3; Table S3) suggesting that mosses are
163 highly sensitive to change.
164
165 The past sensitivity of moss growth and mass accumulation rates to temperature (see Experimental
166 Procedures) rise was used to provide a first order estimate of likely responses to future warming.
167 Regionally averaged sensitivity was estimated by calculating rates of change for moss growth and
168 mass accumulation at all sites from 1950 – 2012 and combining these with decadal temperature
169 trends for the AP derived from reanalysis data [34]. This suggested that moss growth rates have
170 increased by 3.2 mm $°C^{-1}$ (range 1.8 – 13.4 mm $°C^{-1}$) and mass accumulation rates by 0.05 g DM cm^{-2}
171 $°C^{-1}$ (range 0.03 – 0.2 g DM cm^{-2} $°C^{-1}$) compared to baseline (i.e. pre-changepoint) mean rates of
172 0.78 mm yr^{-1} and 0.009 g DM cm^{-2} yr^{-1} respectively (Table S4). Although these estimates are variable

between and within sites and constrained by chronological precision, they suggest that moss bank growth and accumulation will be highly sensitive to future temperature change.

The sensitivity of this response is moderated by moisture availability, but our spatially-consistent records covering the last 150 years suggest that the effect of temperature is dominant. Projections of future temperature increases for the Antarctic Peninsula are subject to very large uncertainties [1], but our data on increased moss growth and increased microbial populations, combined with increased fungal diversity [39] and vascular plant distribution [11], all indicate that terrestrial plant communities and soils will undergo substantial alteration even with only modest further increases in temperature. These changes, combined with increased ice-free land areas from glacier retreat [30], will drive large scale alteration to the biological functioning, appearance and landscape of the AP over the rest of the 21st century and beyond. Whilst the biogeographical isolation and low vascular plant species diversity [40] of Antarctica mean we must think differently about the two polar regions, a greening of the fringes of the Antarctic may already be underway, similar to the well-documented and extensive greening of the Arctic [20].

Author contributions

DJC, DAH, PC and HG conceived the research project and secured funding; fieldwork was completed by MJA, DJC, DAH, PC and JR; laboratory work was completed by MJA, TPR and JR; data analyses were completed by MJA, JR and TPR; MJA and DJC wrote the manuscript with assistance from TPR and all authors provided editorial advice and contributed to revisions.

Acknowledgements

This research was funded by the UK Natural Environment Research Council (NERC) Antarctic Funding Initiative grant 11/05 (NE/H014896/1) held by DJC, DAH, PC and HG. PC, DAH and JR contribute to the BAS 'Polar Science for Planet Earth' research programme. Radiocarbon analyses were supported by allocation number 1605.0312 from the NERC Radiocarbon Facility, East Kilbride. We gratefully acknowledge Professor Melanie Leng at the NERC Isotope Geosciences Laboratory for assistance with isotope measurements and Nicole Sanderson at the University of Exeter for assistance with ^{210}Pb age modelling. Sample collection was supported by HMS Protector and HMS Endurance; many thanks to Iain Rudkin and Ashly Fusiarski for fieldwork support.

References

1. Turner, J., Barrand, N.E., Bracegirdle, T.J., Convey, P., Hodgson, D.A., Jarvis M, Jenkins, A., Marshall, G.J., Meredith, M.P., Roscoe, H. and Shanklin, J. (2014). Antarctic Climate Change and the Environment: An Update. Polar Rec. *50*, 237–259.
2. Turner, J., Bindschadler, R., Convey, P., di Prisco, G., Fahrbach, E., Gutt, J., Hodgson, D.A., Mayewski, P. and Summerhayes, C. (2009). Antarctic climate change and the environment. (Cambridge: Scientific Committee on Antarctic Research).
3. Vaughan, D.G., Marshall, G.J., Connolley, W.M., Parkinson, C., Mulvaney, R., Hodgson, D.A., King, J.C., Pudsey, C.J. and Turner, J. (2003). Recent rapid regional climate warming on the Antarctic Peninsula. Clim. Change *60*, 243–274.
4. Turner, J., Lu, H., White, I., King, J.C., Phillips, T., Hosking, J.S., Bracegirdle, T.J., Marshall, G.J., Mulvaney, R. and Deb, P. (2016). Absence of 21st century warming on Antarctic Peninsula consistent with natural variability. Nature *535*, 411–415.
5. Turner, J., Lachlan-Cope, T.A., Colwell, S. and Marshall, G.J. (2005). A positive trend in western Antarctic Peninsula precipitation over the last 50 years reflecting regional and Antarctic-wide atmospheric circulation changes. Ann. Glaciol. *41*, 85–91.

6. Kirchgäßner, A. (2011). An analysis of precipitation data from the Antarctic base Faraday/Vernadsky. Int. J. Climatol. *31*, 404–414.
7. Abram, N.J., Mulvaney, R., Wolff, E.W., Triest, J., Kipfstuhl, S., Trusel, L.D., Vimeux, F., Fleet, L. and Arrowsmith, C. (2013). Acceleration of snow melt in an Antarctic Peninsula ice core during the Twentieth Century. Nat. Geosci. *6*, 404–411.
8. Moreau, S., Mostajir, B., Bélanger, S., Schloss, I.R., Vancoppenolle, M., Demers, S. and Ferreyra, G.A. (2015). Climate change enhances primary production in the western Antarctic Peninsula. Glob. Change Biol. *21*, 2195–2205.
9. Convey, P. and Smith, R.I.L. (2006). Responses of terrestrial Antarctic ecosystems to climate change. Plant Ecol. *182*, 1–10.
10. Parnikoza, I., Convey, P., Dykyy, I., Trokhymets, V., Milinevsky, G., Tyschenko, O., Inozemtseva, D. and Kozeretska, I. (2009). Current status of the Antarctic herb tundra formation in the central Argentine Islands. Glob. Change Biol. *15*, 1685–1693.
11. Cannone, N., Guglielmin, M., Convey, P., Worland, M.R. and Favero Longo, S.E. (2016). Vascular plant changes in extreme environments: effects of multiple drivers. Clim. Change 134, 651–665.
12. Royles, J., Amesbury, M.J., Roland, T.P., Jones, G.D., Convey, P., Griffiths, H., Hodgson, D.A. and Charman, D.J. (2016). Moss stable isotopes (carbon-13, oxygen-18) and testate amoebae reflect environmental inputs and microclimate along a latitudinal gradient on the Antarctic Peninsula. Oecologia *181*, 931–945.
13. Royles, J. and Griffiths, H. (2015). Invited review: climate change impacts in polar regions: lessons from Antarctic moss bank archives. Glob. Change Biol. *21*, 1041–1057.
14. Royles, J., Amesbury, M.J., Convey, P., Griffiths, H., Hodgson, D.A., Leng, M.J. and Charman, D.J. (2013). Plants and soil microbes respond to recent warming on the Antarctic Peninsula. Curr. Biol. *23*, 1702–1706.
15. Royles, J., Ogée, J., Wingate, L., Hodgson, D.A., Convey, P. and Griffiths, H. (2012). Carbon

247 isotope evidence for recent climate-related enhancement of CO_2 assimilation and peat
248 accumulation rates in Antarctica. Glob. Change Biol. *18*, 3112–3124.
249 16. Jassey, V.E., Chiapusio, G., Binet, P., Buttler, A., Laggoun-Défarge, F., Delarue, F., Bernard, N.,
250 Mitchell, E.A.D., Toussaint, M-L, Francez, A-J. and Gilbert, D. (2013). Above- and belowground
251 linkages in Sphagnum peatland: Climate warming affects plant-microbial interactions. Glob.
252 Change Biol. *19*, 811–823.
253 17. Gilbert, D., Amblard, C., Bourdier, G. and Francez, A. (1998). The microbial loop at the surface of
254 a peatland: structure, function and impact of nutrient input. Microb. Ecol. *35*, 83–93.
255 18. Mitchell, E.A.D., Gilbert, D., Buttler, A.J., Amblard, C., Grosvernier, P., Gobat, J. (2003). Structure
256 of microbial communities in *Sphagnum* peatlands and effect of atmospheric carbon dioxide
257 enrichment. Microb. Ecol. *46*, 187–199.
258 19. Fenton, J.H.C. (1980). The rate of peat accumulation in Antarctic moss banks. J. Ecol. *68*, 211–
259 228.
260 20. Ju, J. and Masek, J.G. (2016). The vegetation greenness trend in Canada and US Alaska from
261 1984-2012 Landsat data. Remote Sens. Environ. 176, 1–16.
262 21. Fenton, J.H.C. and Smith, R.I.L. (1982). Distribution, composition and general characteristics of
263 the moss banks of the maritime Antarctic. BAS Bull. *51*, 215–236.
264 22. Roads, E., Longton, R.E. and Convey, P. (2014). Millennial timescale regeneration in a moss from
265 Antarctica. Curr. Biol. *24*, R222–R223.
266 23. Morris, E,M, and Vaughan, D.G. (2003). Spatial and temporal variation of surface temperature
267 on the Antarctic Peninsula and the limit of viability of ice shelves. In Antarctic Peninsula
268 Climate Variability: Historical and Palaeoenvironmental Perspectives, E. Domack et al., eds.
269 (Washington DC: American Geophyiscal Union Antarctic Research Series Volume 79). pp. 61-
270 68.
271 24. Hughes, K.A., Worland, M.R., Thorne, M.A.S. and Convey, P. (2013). The non-native chironomid

272 Eretmoptera murphyi in Antarctica: Erosion of the barriers to invasion. Biol. Invasions *15*, 269-
273 281.
274 25. Jones, J.M., Gille, S.T., Goosse, H., Abram, N.J., Canziani, P.O., Charman, D.J., Clem, K.R., Crosta,
275 X., de Lavergne, C., Eisenman, I. et al. (2016). Assessing recent trends in high-latitude Southern
276 Hemisphere surface climate. Nat. Clim. Change *6*, 917–926.
277 26. Mayewski, P.A., Carleton, A.M., Birkel, S.D., Dixon, D., Kurbatov, A.V., Korotkikh, E., McConnell, J.,
278 Curran, M., Cole-Dai, J., Jiang, S. et al. (2017). Ice core and climate reanalysis analogs to predict
279 Antarctic and Southern Hemisphere climate changes. Quat. Sci. Rev. *155*, 50–66.
280 27. Mulvaney, R., Abram, N.J., Hindmarsh, R.C.A., Arrowsmith, C., Fleet, L., Triest, J., Sime, L.C.,
281 Alemany, O. and Foord, S. (2012). Recent Antarctic Peninsula warming relative to Holocene
282 climate and ice shelf history. Nature *489*, 141–145.
283 28. Cook, A.J. and Vaughan, D.G. (2010). Overview of areal changes of the ice shelves on the
284 Antarctic Peninsula over the past 50 years. Cryosph. *4*, 77–98.
285 29. Cook, A.J., Fox, A.J., Vaughan, D.G. and Ferrigno, J.G. (2015). Retreating glacier fronts on the
286 Antarctic Peninsula over the past half-century. Science *308*, 541–544.
287 30. Cook, A.J., Holland, P.R., Meredith, M.P., Murray, T., Luckman, A. and Vaughan, D.G. (2016).
288 Ocean forcing of glacier retreat in the western Antarctic Peninsula. Science *353*, 283–286.
289 31. Bentley, M.J., Hodgson, D.A., Smith, J.A., Cofaigh, C., Domack, E.W., Larter, R.D., Roberts, S.J.,
290 Brachfeld, S., Leventer, A., Hjort, C. et al. (2009). Mechanisms of Holocene palaeoenvironmental
291 change in the Antarctic Peninsula region. The Holocene *19*, 51–69.
292 32. Seddon, A.W.R., Mackay, A.W., Baker, A.G., Birks, H.J.B., Breman, E., Buck, C.E., Ellis, E.C., Froyd,
293 C.A., Gill, J.A., Gillson, L. et al. (2014). Looking forward through the past: Identification of 50
294 priority research questions in palaeoecology. J. Ecol. *102*, 256–267.
295 33. Walther, G.R., Post, E., Convey, P., Menzel, A., Parmesan, C., Beebee T.J.C., Fromentin, J-M.,
296 Hoegh-Guldberg, O. and Bairlein, F. (2002). Ecological responses to recent climate change.

297 Nature *416*, 389–395.
298 34. Nicolas, J.P. and Bromwich, D.H. (2014). New reconstruction of Antarctic near-surface
299 temperatures: Multidecadal trends and reliability of global reanalyses. J. Clim. *27*, 8070–8093.
300 35. Turner, J., Colwell, S.R., Marshall, G.J., Lachlan-Cope, T.A., Carleton, A.M., Jones, P.D., Lagun, V.,
301 Reid, P.A. and Iagokina, S. (2005). Antarctic climate change during the last 50 years. Int. J.
302 Climatol. *25*, 279–294.
303 36. Convey, P., Block, W., Peat, H.J. (2003). Soil arthropods as indicators of water stress in Antarctic
304 terrestrial habitats? Glob. Change Biol. *9*, 1718–1730.
305 37. Mayewski, P.A., Bracegirdle, T., Goodwin, I., Schneider, D., Bertler, N.A.N., Birkel, S., Carleton, A.,
306 England, M.H., Kang, J-H., Khan, A. et al. (2015). Potential for Southern Hemisphere climate
307 surprises. J. Quat. Sci. *30*, 391–395.
308 38. Bramley-Alves, J., Wanek, W., French, K., Robinson, S.A. (2015). Moss $\delta^{13}C$: An accurate proxy for
309 past water environments in polar regions. Glob Chang Biol *21*, 2454–2464.
310 39. Newsham, K.K., Hopkins, D.W., Carvalhais, L.C., Fretwell, P.T., Rushton, S.P., O'Donnell, A.G. and
311 Dennis, P.G. (2015). Relationship between soil fungal diversity and temperature in the maritime
312 Antarctic. Nat. Clim. Change *6*, 182–186.
313 40. Cavieres, L.A., Saez, P., Sanhueza, C., Sierra-Almeida, A., Rabert, C., Corcuera, L.J., Alberdi, M.
314 and Bravo, L.A. (2016). Ecophysiological traits of Antarctic vascular plants: their importance in
315 the responses to climate change. Plant Ecol. *217*, 343–358.
316 41. Amesbury, M.J., Barber, K.E. and Hughes, P.D.M. (2011). The methodological basis for fine-
317 resolution, multi-proxy reconstructions of ombrotrophic peat bog surface wetness. Boreas *40*,
318 161–174.
319 42. Appleby, P.G. and Oldfield, F. (1978). The calculation of lead-210 dates assuming a constant
320 rate of supply of unsupported 210Pb to the sediment. Catena *5*, 1–8.
321 43. Blaauw, M. (2010). Methods and code for "classical" age-modelling of radiocarbon sequences.

322 Quat. Geochronol. *5*, 512–518.
323 44. Loader, N.J., Robertson, I., Barker, A.C., Switsur, V.R. and Waterhouse, J.S. (1997). An improved
324 technique for the batch processing of small wholewood samples to α-cellulose. Chem. Geol.
325 *136*, 313–317.
326 45. Rubino, M., Etheridge, D.M., Trudinger, C.M., Allison, C.E., Battle, M.O., Langenfelds, R.L., Steele,
327 L.P., Curran, M., Bender, M., White, J.W.C. et al. (2013). A revised 1000 year atmospheric $\delta^{13}C$-
328 CO_2 record from Law Dome and South Pole, Antarctica. J. Geophys. Res. Atmos. *118*, 8482–
329 8499.
330 46. Booth, R.K., Lamentowicz, M. and Charman, D.J. (2010). Preparation and analysis of testate
331 amoebae in peatland palaeoenvironmental studies. Mires Peat *7*, 1–7.
332 47. Killick, R. and Eckley, I. (2013). changepoint: An R Package for changepoint analysis. J. Stat.
333 Softw. *58*, 1-15.
334

335 **Figure legends**

336 **Figure 1:** Regional map of the Antarctic Peninsula showing moss bank sites (black dots are new
337 locations used in this analysis, grey dot is previously published [14]) and meteorological records
338 (white dots) of recent mean annual temperature, with decadal trends [35]. Approximate position of
339 -5°C and -9°C isotherms [23,24] illustrate lack of significant latitudinal temperature gradients over
340 western AP study area.
341

342 **Figure 2:** Time series of proxies for moss productivity ($\Delta^{13}C$) and soil microbial activity (testate
343 amoeba productivity) alongside moss growth and mass accumulation rates for all sites/cores. Green
344 lines represent the mean values of samples before and after each identified changepoint. All
345 changepoints are significant at a confidence value >0.98. Years shown for changepoint occurrence
346 represent the min – max range of the modelled date of the first sample in the new state. Red arrows

show direction of primary recent trend in time series where significant changepoints were not identified. See Figure S2 for results using CUSUM approach to changepoint detection. Note differing y-axis scales. For references to colour, readers are referred to the online version of the manuscript.

Figure 3: Summary changepoint data for all proxies with the exception of $\Delta^{13}C$. Coloured lines represent different sites/cores/proxies; horizontal lines represent the mean values of all samples before and after the changepoint, vertical line shows timing of state change. Dashed vertical line indicates 1950. Spot data in background are individual times series from all sites/cores/proxies. For references to colour, readers are referred to the online version of the manuscript.

Figure 4: Pre- (left hand) and post- (right hand) 1950 boxplots for all proxies, averaged across all sites/cores. See Figure S1 for complete boxplot matrix.

STAR methods

EXPERIMENTAL MODEL AND SUBJECT DETAILS

N/A

METHOD DETAILS

Moss bank core collection and sampling

Cores were collected in January 2012 (Elephant Island and Ardley Island) and January 2013 (Green Island). Sites were selected to access the deepest and oldest records available, whilst ensuring as complete spatial coverage of the AP as possible given the sporadic locations in which moss banks grow. Cores were carefully cut and removed by hand from non-permafrost near-surface sediments and stored at -20°C. Frozen core sections were sub-sampled at 5 mm resolution using a microtome

372 slicer [41]. All information on the Lazarev Bay site has been previously published [14] and data are
373 included here to extend the spatial transect.
374
375 **Chronology**
376 Age-depth models were developed from conventional and post-bomb ^{14}C and alpha-spectrometry
377 ^{210}Pb. All ^{14}C dates were measured on pure moss fragments. Raw ^{14}C dates and ^{210}Pb ages derived
378 from a constant rate of supply model [42] were entered into the R package 'clam' [43] to develop
379 smooth spline models using the minimum smoothing value (lower values resulting in more flexible
380 models) at which age reversals did not occur in the majority of model iterations. All other settings
381 were default. Moss growth rates were calculated automatically during the age-depth modelling
382 process and therefore reflect the smoothing inherent in the age-depth model. Mass accumulation
383 rates (g DM cm^{-2} yr^{-1}) were calculated using the depth, modelled ages and bulk density values for
384 consecutive samples; bulk density (g cm^{-3}) was calculated by freeze drying samples of known volume.
385 In one core (ARD3) it was not possible to derive a complete bulk density profile due to an air pocket
386 within the core, resulting in a discontinuous record of mass accumulation rates. Details of all ^{14}C and
387 ^{210}Pb dates and age-depth models are given in Table S2.
388
389 **Carbon stable isotopes**
390 Cellulose was extracted from moss samples using a standard protocol [44]. For $\delta^{13}C$ analysis, 1 mg
391 samples of freeze-dried α-cellulose were transferred to tin capsules and measured at the NERC
392 Isotope Geoscience Laboratory (British Geological Survey) by combustion in a furnace connected on-
393 line to a dual inlet isotope ratio mass spectrometer. Isotope ratios ($^{13}C/^{12}C$) were referenced to the
394 VPDB scale using within-run standards. Raw $\delta^{13}C$ values were converted to carbon isotopic
395 discrimination ($\Delta^{13}C$) by reference to age depth models and records of atmospheric ^{13}C in Antarctica

[45]. Moss bank $\Delta^{13}C$ represents a proxy for photosynthetic assimilation rate [14,15], with high discrimination values reflecting optimal hydration and photosynthetic conditions [13,15].

Testate amoeba analysis

Testate amoebae were used as a proxy for microbial productivity [14]. Samples were prepared according to standard methodologies [46], with the size fraction between 300 and 15 µm retained for microscopic analysis. Volumetric concentration values (tests cm^{-3}) were calculated by the addition of an exotic spore marker, with concentration per unit surface area over time (tests cm^{-2} yr^{-1}) calculated with reference to the depths, modelled ages and volumetric concentration values of consecutive samples. Minimum counts of 25 individuals were accepted for statistical analysis due to extremely low concentration in some samples.

Climate data

AP climate station temperature data (Figure 1) were downloaded from the SCAR (Scientific Committee on Antarctic Research) READER (REference Antarctic Data for Environmental Research) database (https://legacy.bas.ac.uk/met/READER/data.html).

QUANTIFICATION AND STATISTICAL ANALYSIS

Changepoint analysis was carried out on all profiles at each site with the exclusion of ARD3 accumulation rate (see Chronology methods). We used the R package 'changepoint' [47] with the cpt.meanvar function to examine concurrent changes in the mean and variance of each time series. We used default settings, which included the 'At Most One Change' method to focus the analysis on the primary changepoint in each time series. Changepoint analysis was carried out on time series data only; ages assigned to changepoints were the min – max ranges of individual samples from the relevant age-depth model. Cumulative sum control chart (CUSUM) profiles for change detection

were calculated manually by plotting the cumulative sum of the differences between individual values and the time series mean against time (Figure S1). Slope directions indicate if data are trending away from or towards the mean value, with change in direction indicating sudden shifts in the mean state. For the sensitivity analysis, we used only growth and mass accumulation rate data as they demonstrate a more direct response to long-term temperature trends, whereas microbial productivity and $\Delta^{13}C$ can be more influenced by site-specific microclimate and microtopography [12]. To assess the sensitivity of these growth parameters to temperature, we calculated decadal rates of change (i.e. change in proxy divided by change in time) from 1950 – 2012 and applied these to a DJF temperature trend from reanalysis data [34], using the temperature trend error to provide a range of possible sensitivity values. Temperature sensitivity estimates are considered to be conservative as 1) they include any recent downturn in proxy values and 2) the DJF trend will be lower than the genuine growing season trend to which moss bank proxies respond, which would include part of the SON and MAM periods, when trends are higher [34].

DATA AND SOFTWARE AVAILABILITY

All software required to perform the analyses described in the 'Quantification and statistical analysis' section is freely available to download for the open source R programme. Raw proxy data is archived at the UK Natural Environment Research Council Polar Data Centre, available via the Discovery Metadata System (https://data.bas.ac.uk/).

ADDITIONAL RESOURCES

N/A

KEY RESOURCES TABLE

REAGENT or RESOURCE	SOURCE	IDENTIFIER
Antibodies		
Bacterial and Virus Strains		
Biological Samples		
Chemicals, Peptides, and Recombinant Proteins		
Critical Commercial Assays		
Deposited Data		
Proxy indices for carbon isotopes, microbial productivity, mass accumulation and moss growth rates, with associated ages.	This paper	Searchable at https://data.bas.ac.uk/
Experimental Models: Cell Lines		
Experimental Models: Organisms/Strains		

Oligonucleotides		
Recombinant DNA		
Software and Algorithms		
‘Changepoint’ R package	Authored by Rebecca Killick, Lancaster University, UK	https://cran.r-project.org/web/packages/changepoint/index.html
Other		

Figure 1

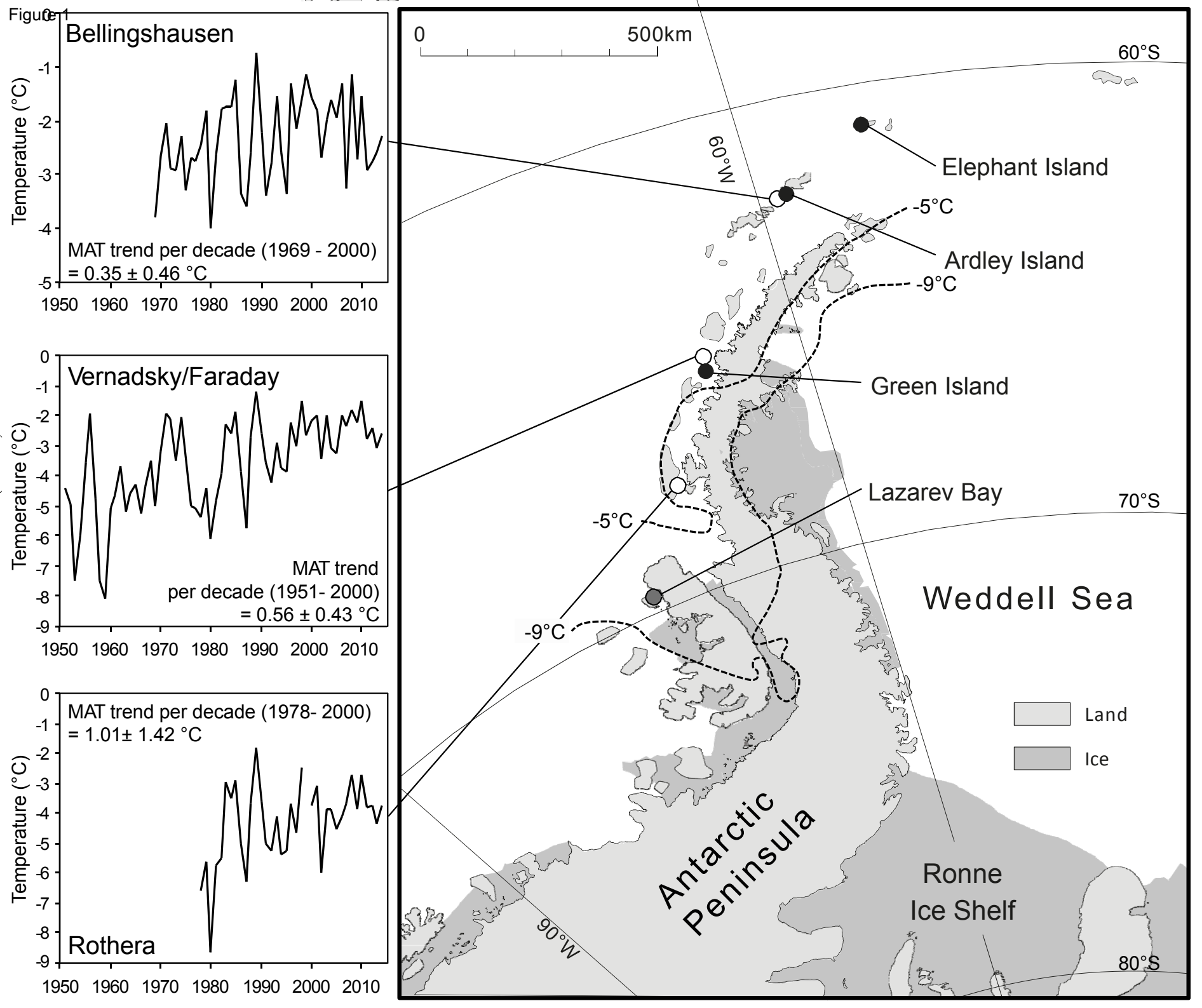
Bellingshausen
Temperature (°C)
MAT trend per decade (1969 - 2000)
= 0.35 ± 0.46 °C
1950 1960 1970 1980 1990 2000 2010
Vernadsky/Faraday
MAT trend
per decade (1951- 2000)
= 0.56 ± 0.43 °C
MAT trend per decade (1978- 2000)
= 1.01± 1.42 °C
Rothera
0
500km
60°S
70°S
80°S
60°W
90°W
Elephant Island
Ardley Island
Green Island
Lazarev Bay
-5°C
-9°C
Weddell Sea
Land
Ice
Antarctic
Peninsula
Ronne
Ice Shelf

Figure 2

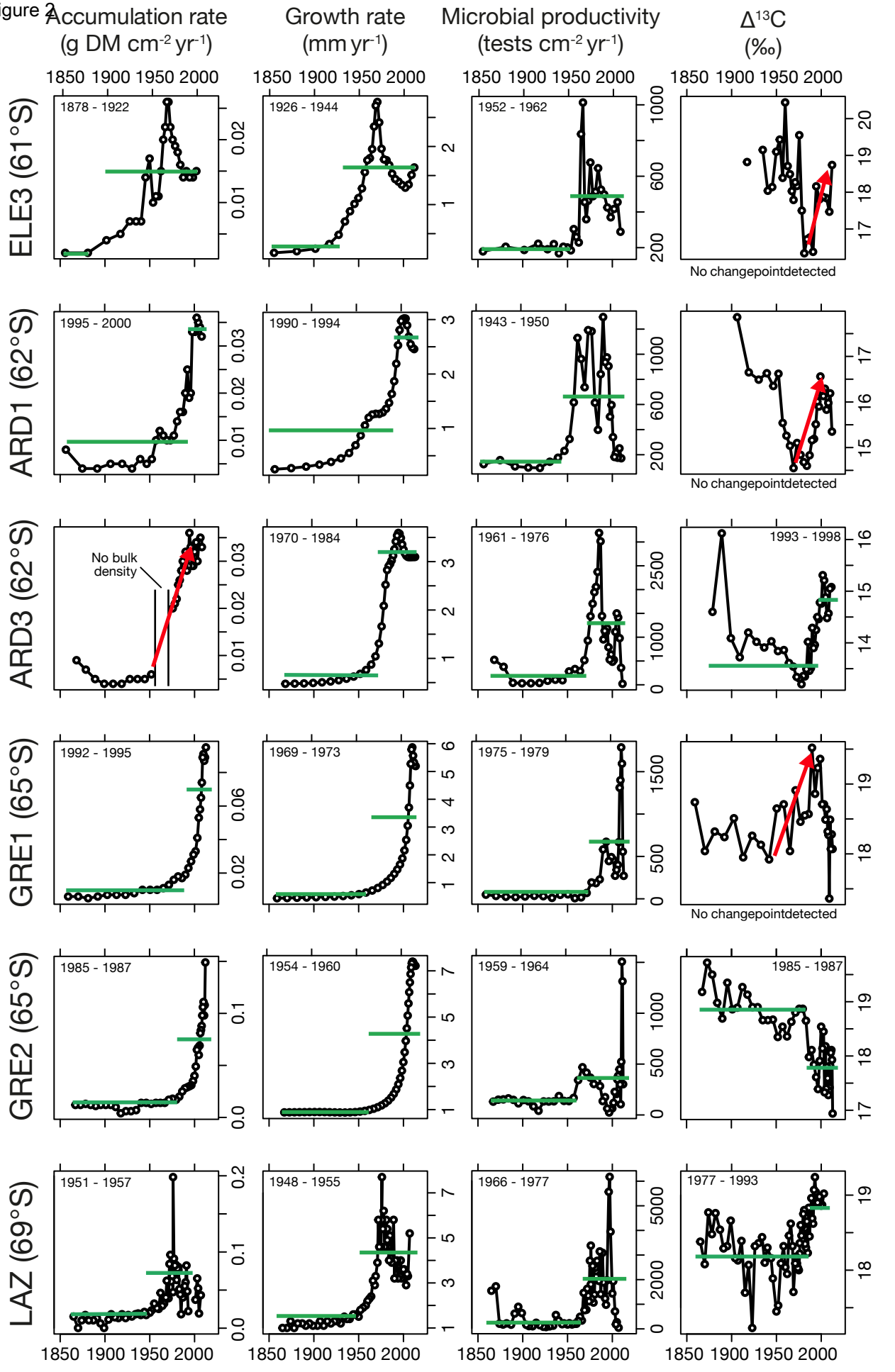
Accumulation rate
(g DM cm-2 yr-1)
Growth rate
(mm yr-1)
Microbial productivity
(tests cm-2 yr-1)
Δ13C
(‰)
ELE3 (61°S)
ARD1 (62°S)
ARD3 (62°S)
GRE1 (65°S)
GRE2 (65°S)
LAZ (69°S)
1878 - 1922
1926 - 1944
1952 - 1962
1995 - 2000
1990 - 1994
1943 - 1950
1970 - 1984
1961 - 1976
1993 - 1998
1992 - 1995
1969 - 1973
1975 - 1979
1985 - 1987
1954 - 1960
1959 - 1964
1985 - 1987
1951 - 1957
1948 - 1955
1966 - 1977
1977 - 1993
No bulk density
No changepointdetected
No changepointdetected
1850 1900 1950 2000

Figure 3

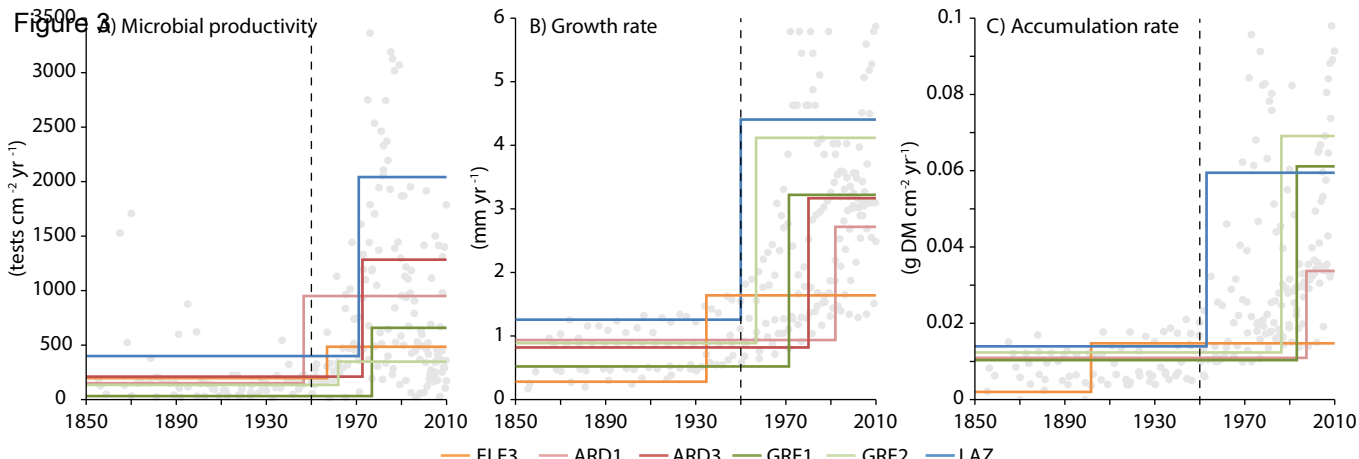
A) Microbial productivity
(tests cm -2 yr -1)
3500
3000
2500
2000
1500
1000
500
0
1850
1890
1930
1970
2010
B) Growth rate
(mm yr -1)
6
5
4
3
2
1
0
1850
1890
1930
1970
2010
C) Accumulation rate
(g DM cm-2 yr-1)
0.1
0.08
0.06
0.04
0.02
0
1850
1890
1930
1970
2010
ELE3
ARD1
ARD3
GRE1
GRE2
LAZ

Figure 4

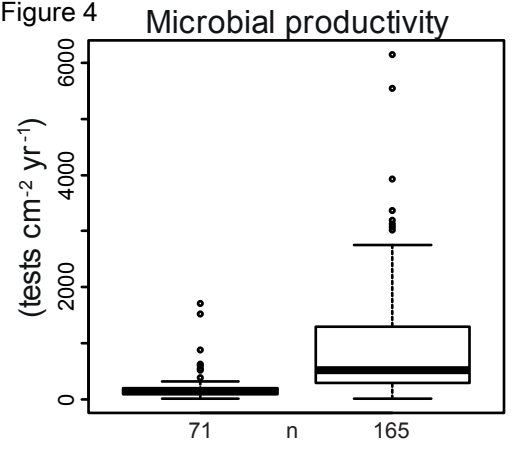
Microbial productivity
(tests cm-2 yr-1)
0
2000
4000
6000
71
n
165

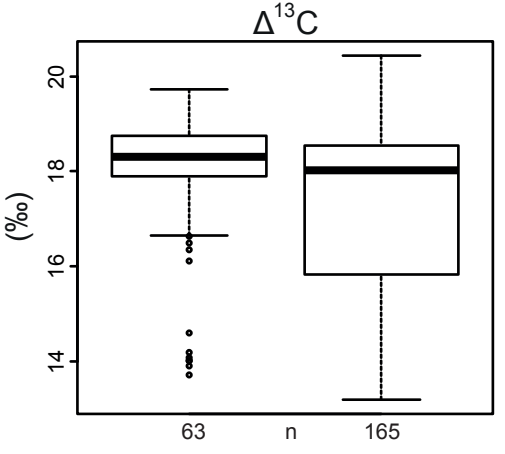
Δ13C
(‰)
14
16
18
20
63
n
165

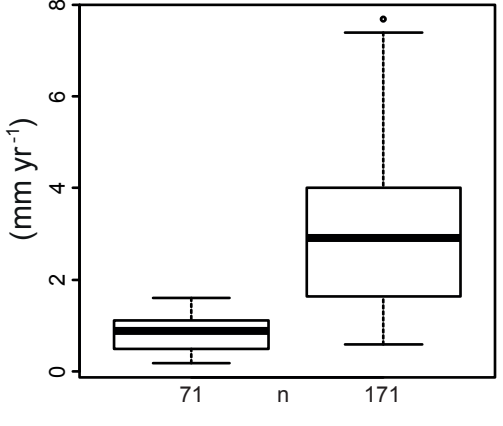
Growth rate
(mm yr-1)
0
2
4
6
8
71
n
171

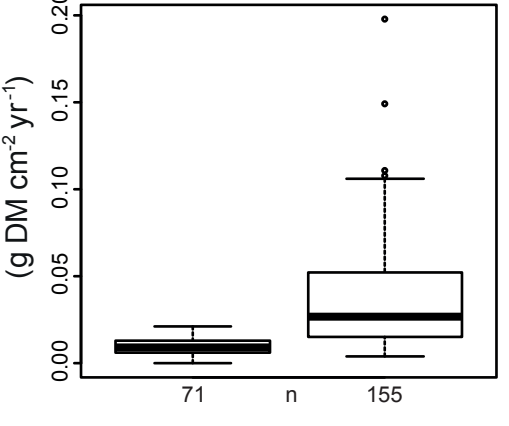
Accumulation rate
(g DM cm-2 yr-1)
0.00
0.05
0.10
0.15
0.20
71
n
155

Figure S1: Pre- (left hand) and post- (right hand) changepoint boxplots for all sites/cores/proxies that exhibited significant changepoints. Missing plots represent sites/cores/proxies where significant changepoints were not identified. ELE = Elephant Island, ARD = Ardley Island, GRE = Green Island, LAZ = Lazarev Bay [14]. Changepoint age for splitting each time series was the 'best' age estimate from the relevant age-depth model (related to Figure 4).

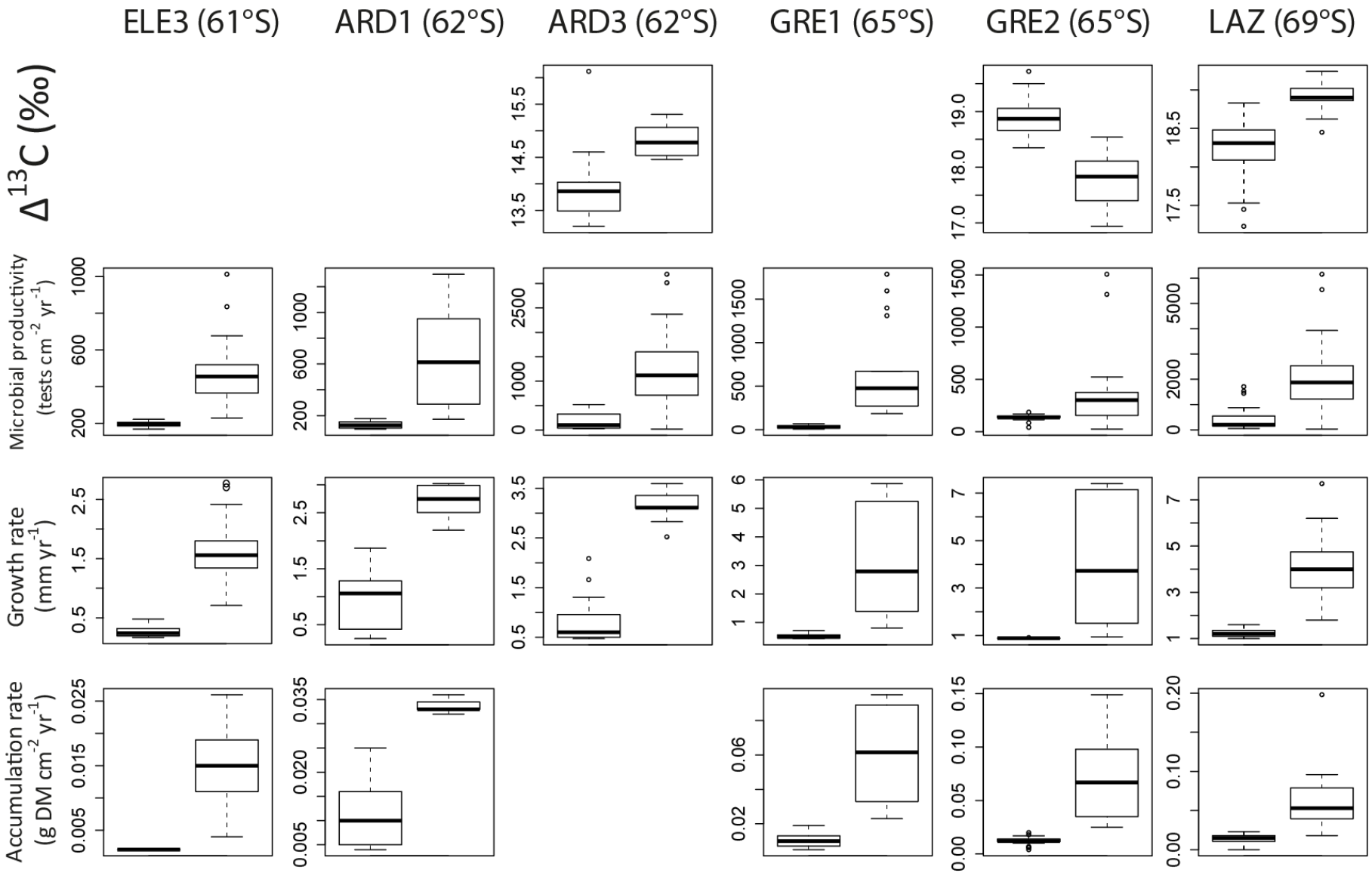

Figure S2: CUSUM plots for all sites/cores/proxies (related to Figure 2). Highlighted red samples indicate a change direction of values with respect to the time series mean; the min – max modelled ages of these samples are shown. For comparison, green vertical shaded areas indicate the min – max ages of significant changepoints. ELE = Elephant Island, ARD = Ardley Island, GRE = Green Island, LAZ = Lazarev Bay [14].

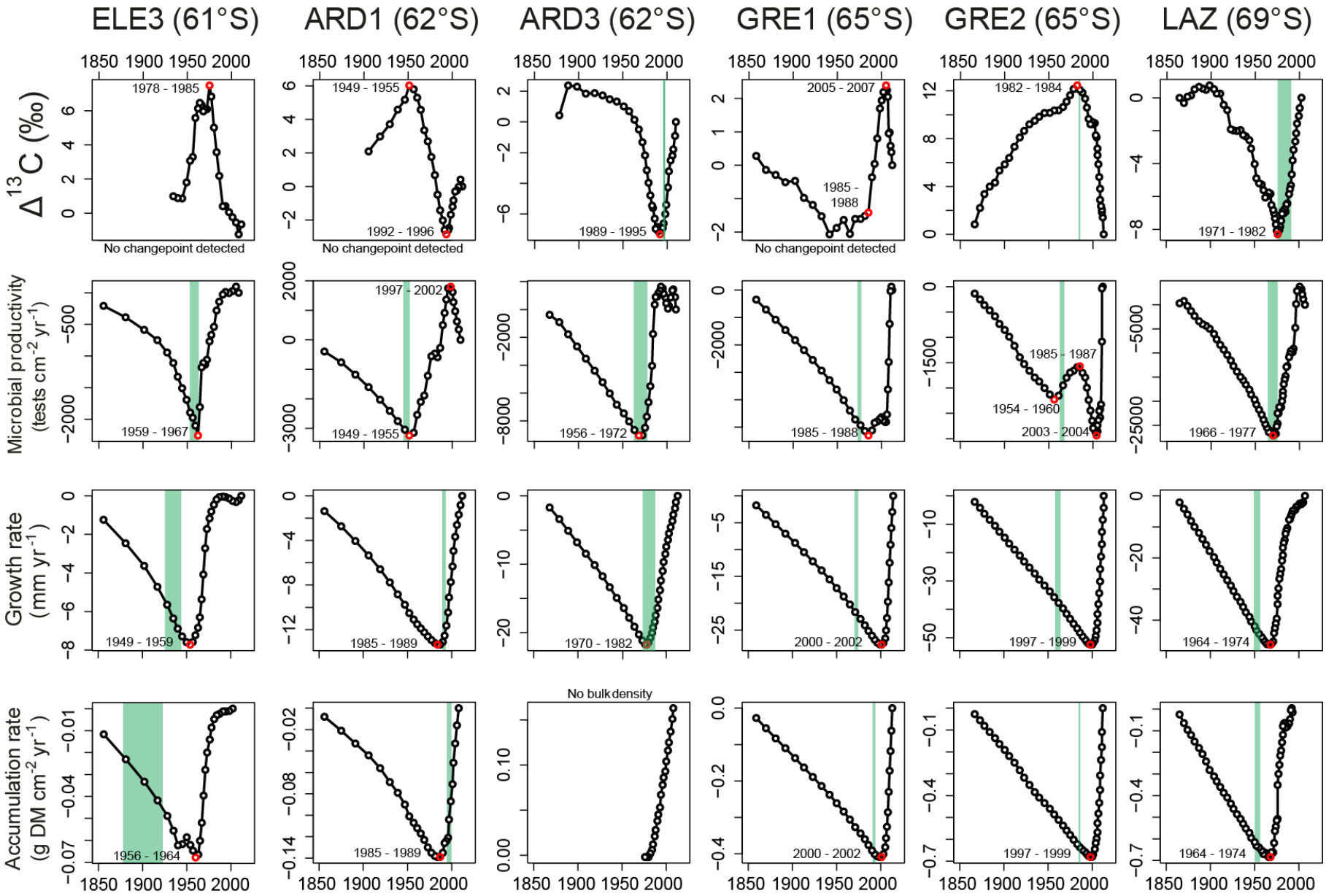

Figure S3: Age-depth models for all cores. A: Elephant Island (ELE3); B, C: Ardley Island (B – ARD1, C – ARD3); D, E: Green Island (D – GRE1, E – GRE2). Black line is 'best' age estimate with error margins shown as grey shading. Blue age distributions are ^{14}C; green are ^{210}Pb (related to STAR methods Chronology section and Table S2).

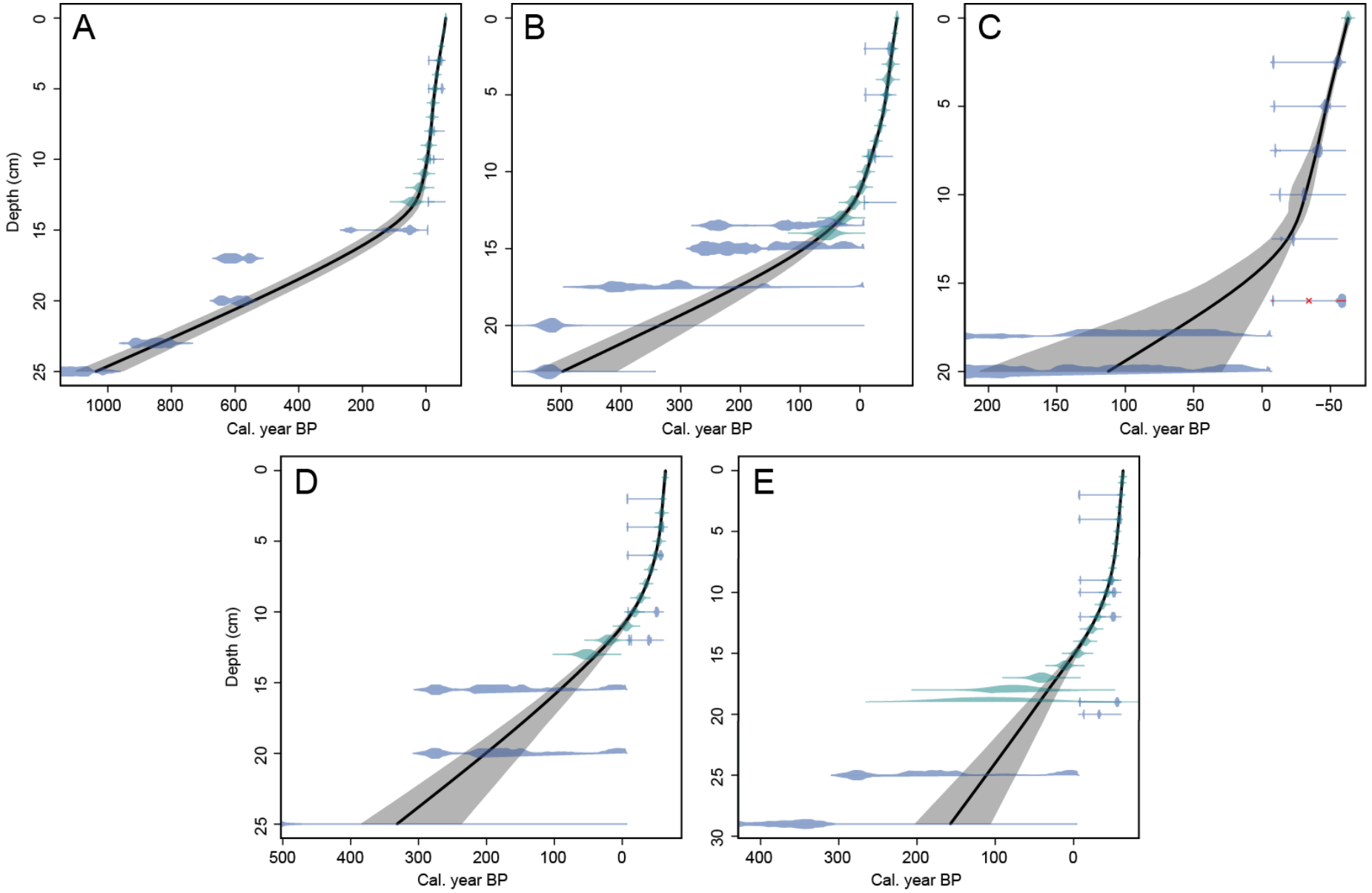

Figure S4: Bulk density and peat humification profiles for all sites and cores. Related to Results 'Moss banks are regional palaeoclimate archives' section.

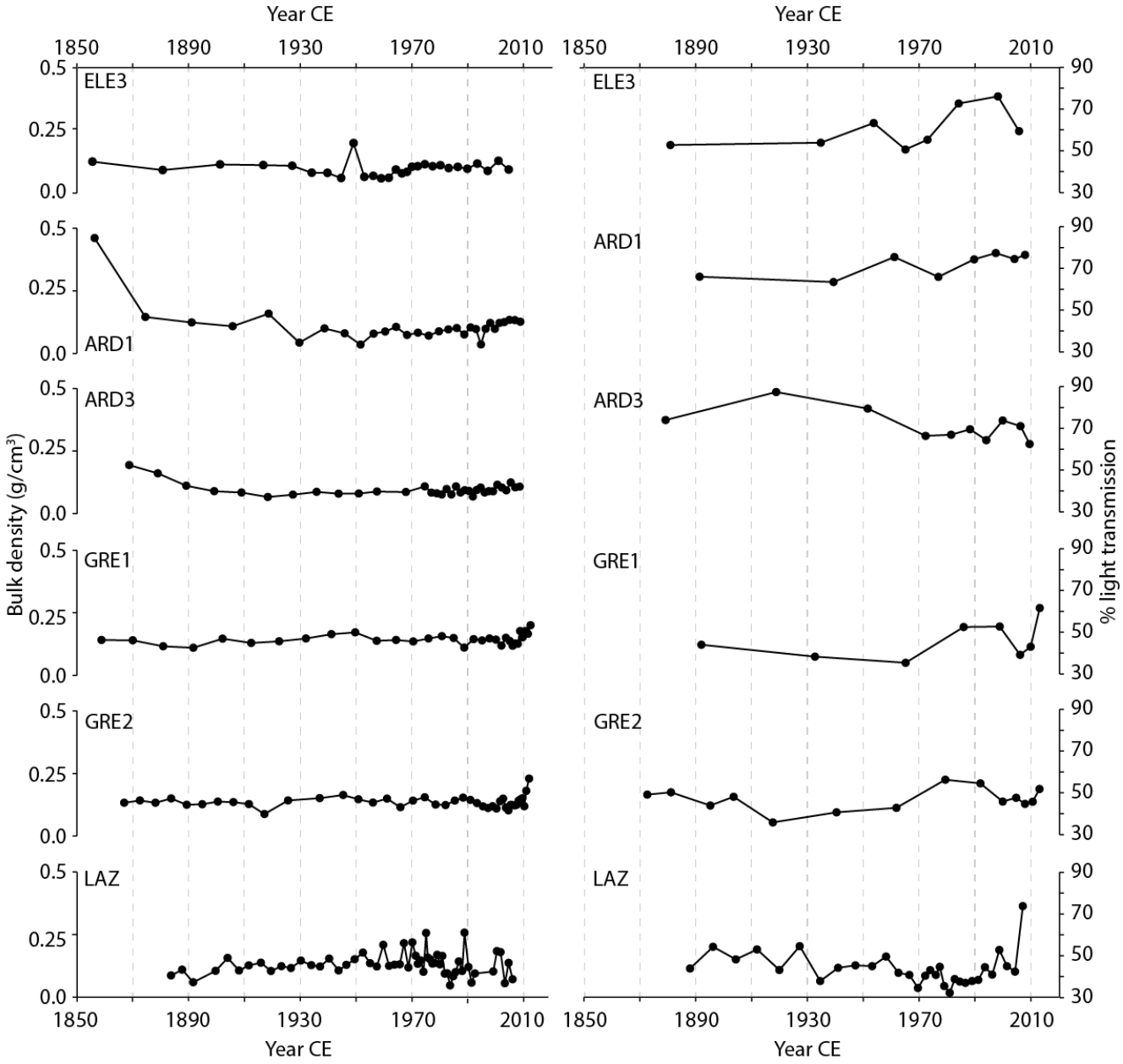

Table S1: Site meta-data for new sites and cores included in this study. Equivalent information for Lazarev Bay is published elsewhere [14]. Related to Results 'Moss banks are regional palaeoclimate archives' section.

Site name	Latitude (°S)	Longitude (°W)	Core code	Total core depth (max. depth analysed in this study)	Number of samples post-1850	Dominant moss type
Elephant Island	61.111	54.824	ELE3	25 cm (15 cm)	30	*Chorisodontium aciphyllum*
Ardley Island	62.213	58.935	ARD1	23 cm (15.5 cm)	31	*Chorisodontium aciphyllum*
Ardley Island	62.213	58.935	ARD3	19 cm (19 cm)	38	*Chorisodontium aciphyllum*
Green Island	65.322	64.151	GRE1	97 cm (16 cm)	32	*Polytrichum strictum*
Green Island	65.322	64.151	GRE2	66 cm (23 cm)	46	*Polytrichum strictum*

Table S2: Chronological results including radiocarbon and alpha spectrometry lead dating results from all sites (ELE = Elephant Island, ARD = Ardley Island, GRE = Green Island). For lead dating, CRS (Constant Rate of Supply – see STAR methods) modelled ages, with error margins, are also included. No lead dating results are included for ARD3 as it was not possible to define the background, unsupported level of ^{210}Pb for that core, precluding model development. *Radiocarbon date omitted from age modelling as reversal (see also Figure S3 C). Dating information relating to Lazarev Bay is published elsewhere [14]. Related to Figure S3 and STAR methods Chronology section.

Site/core code	Sample depth (cm)	Radiocarbon identifier	^{14}C enrichment (absolute % modern carbon, ± 1σ)	Conventional ^{14}C age (± 1σ)	Pb-210 activity (Bq/kg)	± error margin	CRS modelled age (year AD)	± error margin
ELE3	1				34.63	1.30	2006	1
ELE3	2				34.68	1.36	1999	2
ELE3	3	SUERC-54332	111.56 ± 0.58		27.00	1.23	1991	3
ELE3	4				27.12	1.11	1984	3
ELE3	5	SUERC-49613	109.66 ± 0.48		23.71	1.11	1978	4
ELE3	6				21.78	1.05	1972	4
ELE3	7				19.04	0.86	1969	4
ELE3	8	SUERC-54333	138.83 ± 0.72		21.28	1.22	1965	4
ELE3	9				22.01	1.23	1959	5
ELE3	10	SUERC-49614	142.59 ± 0.63		21.08	1.02	1952	6
ELE3	11				21.92	1.30	1944	7
ELE3	12				23.40	1.40	1930	9
ELE3	13	SUERC-54334	103.10 ± 0.51		22.26	1.15	1906	14
ELE3	15	SUERC-49616		43 ± 37				
ELE3	17	SUERC-54335		589 ± 39				
ELE3	20	SUERC-49617		628 ± 37				
ELE3	23	SUERC-54336		953 ± 39				
ELE3	25	SUERC-46889		1175 ± 37				
ARD1	1				56.21	3.18	2008	1
ARD1	2	SUERC-54337	110.25 ± 0.55		47.95	3.13	2004	2
ARD1	3				60.56	2.78	2001	2
ARD1	4				60.25	3.45	1997	2
ARD1	5	SUERC-49620	113.52 ± 0.53		56.24	2.95	1994	2
ARD1	6				67.63	3.15	1990	2
ARD1	7				76.35	3.26	1984	2
ARD1	8				76.71	3.77	1977	2
ARD1	9	SUERC-54338	139.23 ± 0.72		58.46	3.54	1968	3
ARD1	10				44.21	2.39	1960	3
ARD1	11				48.99	2.27	1952	4
ARD1	12	SUERC-49621	102.37 ± 0.48		41.72	2.35	1939	5
ARD1	13				30.12	2.28	1919	8
ARD1	13.5	SUERC-54339	99.24 ± 0.51					
ARD1	14				22.46	2.02	1894	13

ARD1	15	SUERC-49622		129 ± 37				
ARD1	17.5	SUERC-54342		272 ± 41				
ARD1	20	SUERC-49623		475 ± 37				
ARD1	23	SUERC-54344		490 ± 37				
ARD3	2.5	SUERC-54345	107.36 ± 0.55					
ARD3	5	SUERC-49624	111.88 ± 0.52					
ARD3	7.5	SUERC-54346	115.65 ± 0.60					
ARD3	10	SUERC-49625	128.24 ± 0.60					
ARD3	12.5	SUERC-54347	146.46 ± 0.76					
ARD3	16*	SUERC-49626	106.21 ± 0.49					
ARD3	18	SUERC-54348		92 ± 41				
ARD3	20	SUERC-44336		139 ± 37				
GRE1	1				14.88	0.84	2010	1
GRE1	2	SUERC-54349	104.30 ± 0.54		14.00	0.75	2008	2
GRE1	3				19.53	1.03	2007	2
GRE1	4	SUERC-54352	105.35 ± 0.54		20.58	1.02	2004	2
GRE1	5				34.81	1.66	1999	2
GRE1	6	SUERC-49627	109.62 ± 0.51		29.17	1.60	1992	2
GRE1	7				23.69	1.11	1985	2
GRE1	8				21.02	1.09	1977	3
GRE1	9				22.81	1.12	1968	3
GRE1	10	SUERC-54353	117.26 ± 0.61		20.08	0.99	1956	4
GRE1	11				24.31	1.23	1929	7
GRE1	12	SUERC-54354	106.82 ± 0.49		10.77	0.73	1898	10
GRE1	15.5	SUERC-49631		175 ± 35				
GRE1	20	SUERC-49632		182 ± 35				
GRE1	25	SUERC-49633		471 ± 37				
GRE2	1				11.01	0.65	2012	1
GRE2	2	SUERC-54359	104.50 ± 0.52		23.12	0.97	2011	1
GRE2	3				21.74	0.89	2009	1
GRE2	4	SUERC-54362	105.21 ± 0.54		22.99	1.00	2008	1
GRE2	5				22.60	1.09	2006	1
GRE2	6				14.19	0.78	2004	1
GRE2	7				25.06	1.05	2003	1
GRE2	8				26.06	1.00	2000	1
GRE2	9	SUERC-49645	110.48 ± 0.51		27.28	1.07	1997	2
GRE2	10	SUERC-49642	109.05 ± 0.51		33.11	1.84	1993	2
GRE2	11				28.89	1.10	1987	2
GRE2	12	SUERC-54363	109.55 ± 0.57		28.03	1.27	1981	2
GRE2	13				23.99	1.05	1973	3
GRE2	14				17.76	0.88	1965	3
GRE2	15				21.92	1.52	1955	4
GRE2	16				20.56	1.05	1939	5

GRE2	17				19.76	0.98	1909	10
GRE2	18				6.59	0.50	1873	26
GRE2	19	SUERC-49646	107.14 ± 0.50		6.79	0.46	1844	61
GRE2	20	SUERC-49644	125.18 ± 0.58					
GRE2	25	SUERC-49647		187 ± 37				
GRE2	29	SUERC-54364		374 ± 41				

Table S3: Summary proxy data for all sites/cores. For changepoint years, see also Figures 2 and 3. Related to Discussion 'Future terrestrial biological change' section.

		ELE3	ARD1	ARD3	GRE1	GRE2	LAZ
Peak values	$\Delta^{13}C$ (‰)	20.44	17.86	16.12	19.52	19.72	19.24
	Testate concentration (tests/cm^2/yr)	1013	1296	3190	1787	1507	6156
	Growth rate (mm/yr)	2.77	3.02	3.59	5.87	7.40	7.70
	Accumulation rate (g DM/cm^2/yr)	0.026	0.036	0.036	0.095	0.149	0.198
Mean all values	$\Delta^{13}C$ (‰)	18.16	15.76	14.17	18.46	18.35	18.39
	Testate concentration (tests/cm^2/yr)	386	523	907	396	266	1220
	Growth rate (mm/yr)	1.41	1.63	2.18	2.21	3.00	3.08
	Accumulation rate (g DM/cm^2/yr)	0.014	0.016	0.022	0.033	0.039	0.040
Mean pre-changepoint	$\Delta^{13}C$ (‰)	-	-	13.88	-	18.89	18.26
	Testate concentration (tests/cm^2/yr)	196	129	211	33	135	399
	Growth rate (mm/yr)	0.28	0.94	0.82	0.52	0.89	1.26
	Accumulation rate (g DM/cm^2/yr)	0.002	0.011	-	0.010	0.012	0.014
Mean post-changepoint	$\Delta^{13}C$ (‰)	-	-	14.83	-	17.78	18.89
	Testate concentration (tests/cm^2/yr)	485	643	1284	659	348	2042
	Growth rate (mm/yr)	1.64	2.72	3.17	3.22	4.12	4.05
	Accumulation rate (g DM/cm^2/yr)	0.015	0.033	-	0.061	0.070	0.060

Table S4: Summary information on proxy trends and rates of change for moss growth and mass accumulation rates for all sites/cores. Rates of change were calculated between the two samples that fell nearest to 1950 and 2012 using the core chronologies. For ARD3, changepoint analysis was not possible due to a break in the record so the values here are the means of the samples before and after the break (see also Figure 2). Figures in parentheses for temperature sensitivity represent the ± error in the AP decadal temperature trend [32]. Related to Discussion 'Future terrestrial biological change' section.

Site/core code	**Rate of change 1950 – 2012 (per °C)**	**Temperature sensitivity (change per °C)**	**Pre-changepoint mean value**	**Post-changepoint mean value**
GROWTH RATE (mm yr^{-1})				
ELE3	0.085	0.5 (0.28 – 2.12)	0.282	1.639
ARD1	0.264	1.55 (0.88 – 6.61)	0.937	2.718
ARD3	0.409	2.41 (1.36 – 10.24)	0.82	3.168
GRE1	0.765	4.5 (2.55 – 19.13)	0.521	3.221
GRE2	1.057	6.22 (3.52 – 26.43)	0.887	4.117
LAZ	0.638	3.75 (2.13 – 15.95)	1.257	4.049
Mean	***0.536***	***3.16 (1.79 – 13.41)***	***0.784***	***3.152***
ACCUMULATION RATE (g DM cm^{-2} yr^{-1})				
ELE3	-0.0004	-0.002 (-0.001 – -0.01)	0.002	0.015
ARD1	0.005	0.03 (0.02 – 0.12)	0.01	0.034
ARD3	0.005	0.03 (0.02 – 0.12)	0.006	0.029
GRE1	0.013	0.07 (0.04 – 0.32)	0.01	0.061
GRE2	0.023	0.13 (0.08 – 0.57)	0.012	0.069
LAZ	0.004	0.02 (0.01 – 0.1)	0.013	0.059
Mean	***0.008***	***0.05 (0.03 – 0.2)***	***0.009***	***0.045***